

244. Ion-Transport Properties of Ionophores in Asymmetric Membranes

by Werner E. Morf, Heidi Ruprecht, and Wilhelm Simon*

Department of Organic Chemistry, Swiss Federal Institute of Technology (ETH), CH-8092 Zürich

(30.VII.85)

The selectivity and the permeability of neutral-carrier-based membranes for substrate ions not only depend on the complexation behavior of the ionophores used, but also on their environment. In asymmetric membranes, ionophores may generally exhibit asymmetric transport properties. Such asymmetric bulk membranes were prepared from two PVC half-membranes incorporating synthetic cation-carriers in different plasticizers. The results of potentiometric and electroanalytical studies are discussed on the basis of a theoretical analysis of the carrier-mediated electrical properties of asymmetric bulk and bilayer membranes.

Introduction. – Virtually, all experimental and theoretical studies concerning the ion transport behavior of ionophores in artificial membranes were restricted either to lipid bilayers of uniform compositions or to homogeneous bulk membrane phases. It is clear that these model membranes behave as symmetric barriers, *i.e.*, the ion permeabilities should be the same in both directions perpendicular to the membrane plane. On the other hand, biological membranes probably show partial asymmetries in composition, as indicated by the preferential location or action of certain membrane proteins (*e.g.* enzymes) on one side. It is, therefore, conceivable that carriers or channels in such asymmetric membranes may generate an anisotropic permeability behavior in the sense that the flux or even the kind of transferred species will depend on the direction of transport. Although the studies by *Läuger* and coworkers [1] [2] and others [3–7] indicate certain asymmetry effects for channels in bilayer membranes (*e.g.* rectification phenomena), there is still no clear evidence for the existence of biological or artificial membranes having an asymmetric permeability selectivity based on ion carriers.

Here, we report on a bulk membrane in which one given ionophore, an electrically neutral carrier ligand, transports cations in the two directions with different selectivity. This asymmetric permeability has been realized for a two-segmented solvent polymeric membrane which offers the ionophore different environments at both membrane/solution interfaces. The asymmetric selectivity behavior observable in potentiometric and electroanalytical studies on such membranes is corroborated by the results of a theoretical analysis.

Theoretical. – Neutral-carrier-based liquid membranes that contain no anionic additives (*e.g.* tetraphenylborates [8–10]) are capable of extracting cations by formation of positively charged carrier complexes and simultaneous formation of anionic sites of low mobility (probably hydroxyl ions trapped in water clusters within the membrane [8] [11]). It was shown that the electromotive behavior and the ion-transport properties of such cation-permselective membranes can be rationalized on the basis of a fixed-site membrane model [8] [12]. Accordingly, it is assumed that the membrane phase contains a given

concentration c of fixed negative charges, leading to the extraction of an equivalent amount of cations, and that a thermodynamic equilibrium exists at each membrane/solution interface, which implies sufficiently high rates of the interfacial ion-exchange reactions. With these assumptions the following relations hold:

$$\sum_m z_m c_m(x) = c(x) \tag{1}$$

$$c_m(0) = K_m(0) a_m' \xi'^{-z_m}; \quad c_m(d) = K_m(d) a_m'' \xi''^{-z_m} \tag{2a} \tag{2b}$$

where $c_m(x)$ are the concentrations of permeating cations M^{z_m} within the membrane ($0 \leq x \leq d$), a_m' and a_m'' are the corresponding ion activities of the two aqueous solutions (') and (") contacting the membrane surfaces at $x = 0$ and $x = d$, respectively, and $K_m(0)$ and $K_m(d)$ are the overall distribution coefficients of the cations at the two membrane boundaries (see below), including the effects of ion-carrier complexation [8–13]. The boundary potential functions ξ' and ξ'' are related to the absolute electrical potentials ϕ as follows:

$$\xi' = \exp\left[\frac{F}{RT}(\phi(0) - \phi')\right]; \quad \xi'' = \exp\left[\frac{F}{RT}(\phi(d) - \phi'')\right] \tag{3a} \tag{3b}$$

where R is the gas constant, T the absolute temperature, and F the Faraday constant.

Since the EMF of an ion-selective electrode cell ($a_m'' = \text{const.}$) mainly reflects the potential difference generated between the sample solution (') and the adjoining membrane surface ($x = 0$), the electrode response is described by the relation

$$E \approx \text{const} + \phi(0) - \phi' = \text{const} + \frac{RT}{F} \ln \xi' \tag{4}$$

where ξ' is obtained from Eqns. 1 and 2a. The following expressions are derived for the EMF response to separate solutions of cations I^{z_i} and J^{z_j}

$$E_i = E_i^\circ + \frac{RT}{z_i F} \ln a_i' \tag{5}$$

$$E_j = E_j^\circ + \frac{RT}{z_j F} \ln [K_{ij}^{\text{Pot}} a_j'^{z_i/z_j}] \tag{6}$$

where E_i° is the standard potential of the cell for solutions of the primary ion, and K_{ij}^{Pot} is the potentiometric selectivity for the interfering ion relative to the primary ion, given by the theoretical result

$$K_{ij}^{\text{Pot}} = \frac{[z_j K_j(0)/c(0)]^{z_i/z_j}}{z_i K_i(0)/c(0)} \quad (\text{normal case}) \tag{7a}$$

Evidently, the ion selectivity of an electrode is generally determined by the ion-extraction properties of the membrane surface that is in contact with the sample solution (here at $x = 0$). If the orientation of the membrane would be reversed and the surface at $x = d$ would be exposed to the sample, one would, therefore, expect a different result for the selectivity coefficient:

$$K_{ij}^{\text{Pot}} = \frac{[z_j K_j(d)/c(d)]^{z_i/z_j}}{z_i K_i(d)/c(d)} \quad (\text{reversed case}) \tag{7b}$$

Of course, the ion selectivities predicted by Eqns. 7a and 7b are identical for homogeneous membranes that show an ideally isotropic behavior. In contrast, asymmetric membranes may exhibit widely different selectivities, depending on their orientation relative to the sample solution.

The present fixed-site membrane model can also be applied to analyze the *electrodialytic ion transport across a neutral carrier membrane*. Corresponding treatments were given earlier for symmetric membrane systems [8] [12] [13] where close correlations between potentiometric and electro-dialytic ion selectivities were established. However, no results were presented so far for asymmetric and inhomogeneous bulk membranes. Generally, the isothermal ion flux J_m of permeating ions M^{z_m} within a macroscopic membrane is described by the *Nernst-Planck* equation:

$$J_m = - \frac{D_m(x) c_m(x)}{RT} \frac{d\tilde{\mu}_m(x)}{dx} \quad (8)$$

with

$$\begin{aligned} \tilde{\mu}_m(x) &= \mu_m^{\circ}(x) + RT \ln a_m(x) + z_m F \phi(x) \\ &= \mu_m^{\circ}(\text{aq}) + RT \ln \frac{c_m(x)}{K_m(x)} + z_m F \phi(x) \end{aligned} \quad (9)$$

where D_m is the ionic diffusion coefficient, $\tilde{\mu}_m$ is the electrochemical potential of the species, μ_m° is its chemical standard potential within the membrane (x) and in the external solutions (aq), respectively; a_m is the activity and c_m the concentration of the permeating ion, ϕ is the local electrical potential, and $K_m(x)$ is a distribution parameter characterizing the hypothetical ion-extraction properties of the membrane zone at x in direct contact with an aqueous solution (for $K_m(0)$ and $K_m(d)$ see also *Eqn. 2*). From *Eqns. 8* and *9* the flux equation can be written in the form:

$$J_m \cdot \exp\left[\frac{z_m F}{RT} \phi(x)\right] = - D_m(x) K_m(x) \cdot \frac{d}{dx} \left\{ \frac{c_m(x)}{K_m(x)} \exp\left[\frac{z_m F}{RT} \phi(x)\right] \right\} \quad (10)$$

Integration of *Eqn. 10* and combination with *Eqns. 2a* and *2b* leads to the following fundamental result for the ion transport through a membrane at steady-state:

$$J_m = \frac{a'_m \exp\left[\frac{z_m F}{RT} \phi'\right] - a''_m \exp\left[\frac{z_m F}{RT} \phi''\right]}{\frac{1}{d} \int_0^d \frac{1}{P_m(x)} \exp\left[\frac{z_m F}{RT} \phi(x)\right] dx} \quad (11)$$

with the permeability function

$$P_m(x) = \frac{D_m(x) K_m(x)}{d} \quad (12)$$

To demonstrate the implications of this relationship, we may use the simplifying assumption that $\phi(x)$ varies linearly and $P_m(x)$ exponentially with x . Then *Eqn. 11* together with *Eqns. 3a* and *3b* leads to the following description of the ion transport, as induced by a transmembrane potential difference $V = \phi' - \phi''$:

$$J_m = \frac{a'_m \exp\left[\frac{z_m F}{RT} V\right] - a''_m}{\frac{\xi'^{z_m}}{P_m(0)} \exp\left[\frac{z_m F}{RT} V\right] - \frac{\xi''^{z_m}}{P_m(d)}} \left(\frac{z_m F}{RT} V + \ln \frac{\xi'^{z_m} P_m(d)}{\xi''^{z_m} P_m(0)} \right) \quad (13)$$

Two limiting cases are discerned for sufficiently high values of the applied voltage (as compared to $RT/F = 25.7$ mV at 25°):

$$J_m = P_m(0) a_m' \xi^{z'-z_m} \frac{z_m F}{RT} V \quad (\text{for } z_m V \gg 0) \tag{14a}$$

$$J_m = P_m(d) a_m'' \xi^{z''-z_m} \frac{z_m F}{RT} V \quad (\text{for } z_m V \ll 0) \tag{14b}$$

It becomes evident that the magnitude of the electrodialytic ion fluxes is mainly controlled by the extraction equilibria at the membrane/solution interface where the permeating species enter the membrane. Thus, if different ions are offered simultaneously in the solution on the entry side, the membrane will show a preferential transport of the species that is also preferred in corresponding ion-selective electrode measurements. For permeating cations I^{z+} and J^{z+} of the same charge and the same external activity, the ratio of electrical transport numbers can be directly correlated with the potentiometric selectivity coefficient (similar correlations are obtained for ions of different charges [8] [12] [13]):

$$\frac{t_j}{t_i} = \frac{J_j}{J_i} = K_{ij}^{Tr} \tag{15}$$

where

$$K_{ij}^{Tr} (V \gg 0) = \frac{P_j(0)}{P_i(0)} \approx K_{ij}^{Pot} \quad (\text{normal}) \tag{16a}$$

$$K_{ij}^{Tr} (V \ll 0) = \frac{P_j(d)}{P_i(d)} = K_{ij}^{Pot} \quad (\text{reversed}) \tag{16b}$$

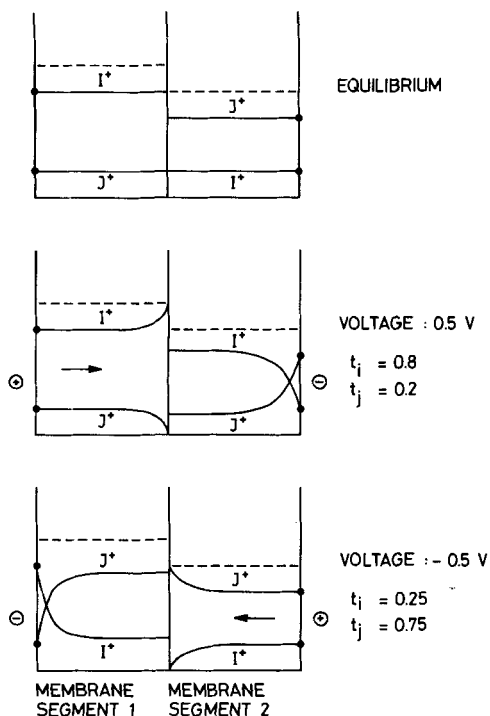


Fig. 1. Calculated concentration profiles for two cations I^+ and J^+ within an asymmetric composite fixed-site membrane at equilibrium and at applied voltages of $+0.5 V$ and $-0.5 V$, respectively. The membrane is interposed between mixed solutions of the cations (1:1). The transport selectivity coefficient K_{ij}^{Tr} is 0.25 for the left half-membrane (segment 1) and 3.0 for the right half-membrane (segment 2). The ratio of the electrical resistances of the two membrane segments is $R_1/R_2 = 1.5$.

Obviously, *Eqns. 16a and 16b* predict that an asymmetric membrane should exhibit two different selectivity characteristics, depending on its orientation and on the direction of ion transport. These expectations are confirmed by model calculations performed on composite fixed-site membranes that consist of two homogeneous membrane segments of differing ion selectivities. The steady-state concentration profiles of permeating cations I^+ and J^+ within such an asymmetric membrane are shown in *Fig. 1*; the computations were based on *Eqn. 10* using the assumption of distribution equilibria at the phase boundaries (see [14]). Since the selectivity coefficients K_{ij} were taken to be 0.25 and 3 for the left and the right membrane segment, respectively, the membrane conditioned at zero-current with equimolar solutions of the two cations finally shows a I^+/J^+ concentration ratio of 4:1 in segment 1 and 1:3 in segment 2 (see *Fig. 1*). At sufficiently high voltages, however, the cations are rapidly driven through the membrane and, as a consequence, the concentration ratios of the permeating species in the major part of the membrane reflect the situation on the respective entry side. Accordingly, the transport numbers are $t_i = 0.8$ and $t_j = 0.2$ for $V \gg 0$, but $t_i = 0.25$ and $t_j = 0.75$ for $V \ll 0$ (*Fig. 1*). These results clearly demonstrate that an asymmetric membrane can facilitate the permeation of ions I^+ in one direction, and of ions J^+ in the opposite direction. Thus a preferential transport of different substrates can be realized by simply changing the direction of the driving force.

It should be noted, however, that *Eqns. 14 and 16* are strictly based on the assumption that the applied voltage drops continuously across the whole interior of the membrane. Similarly, the model calculations summarized in *Fig. 1* were carried out for two membrane segments having a resistance ratio of 3:2 (left:right). This implies, of course, that the ion permeabilities $P_m(x)$ are not strongly disparate at different locations x of the membrane. In contrast, if a given region of the membrane shows extremely low ion permeabilities P_m^{\min} , nearly the whole voltage drop will arise within this high-resistivity barrier and, correspondingly, the term $1/P_m^{\min}$ will finally dominate in the denominator of *Eqn. 11*. In this case, the transport selectivity between cations I^{z+} and J^{z+} becomes:

$$K_{ij}^{\text{Tr}} = \frac{P_j^{\min}}{P_i^{\min}} \quad (\text{for } V \gg 0 \text{ and } V \ll 0) \quad (17)$$

Asymmetric membranes of this type will still exhibit two different selectivity patterns in potentiometric studies (see *Eqns. 7a and 7b*), but they apparently mimic symmetric

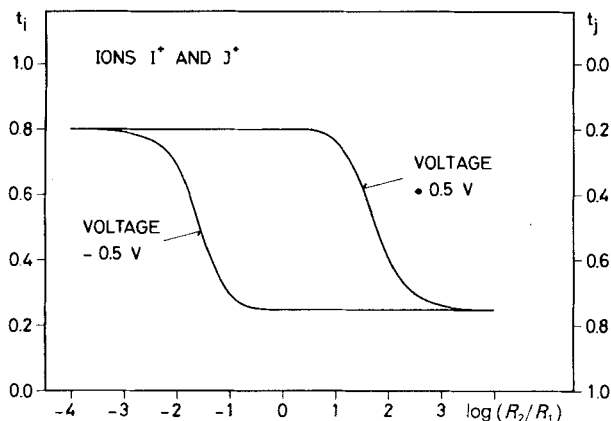


*Fig. 2. Calculated transport numbers for two cations I^+ and J^+ in electro dialysis on asymmetric model membranes (see *Fig. 1*). The resistance ratio R_2/R_1 of the two half-membranes was varied.*

behavior in electroalytic ion-transport experiments. This is underscored in *Fig. 2* by the results of model calculations performed on the two-segmented membrane. The same parameters as in *Fig. 1* were used except that the ratio R_2/R_1 of the electric resistances of the right and the left membrane segment was varied. *Fig. 2* illustrates that, for $R_1 \gg R_2$ or $R_1 \ll R_2$, the transport numbers of the ions approximate the same values as if the high-resistance membrane region were on both sides in direct contact with the external solutions.

Whereas the ion-transport behavior of bulk membrane phases can be well understood on the basis of the generalized *Nernst-Planck* equation (*Eqn. 11*), the *ion fluxes across biological membranes or artificial bilayers* are preferably described by an *Eyring-type* formalism which treats the membrane as a series of N internal and 2 interfacial activation energy barriers [8] [15]:

$$J_m = \frac{a'_m \exp\left[\frac{z_m F}{RT} \phi'\right] - a''_m \exp\left[\frac{z_m F}{RT} \phi''\right]}{\frac{h}{kTl_m} \sum_{n=1}^{N+2} \exp[f_m(n)]} \tag{18}$$

Here h and k are the *Planck* and the *Boltzmann* constant, respectively, l_m is the distance between the interfacial barrier and the neighboring first barrier of the aqueous solution, and $f_m(n)$ is a dimensionless function characterizing the energy at the top of the n -th activation barrier ($\Delta G_m^*(n)$ is the free energy of activation relative to the aqueous phase):

$$f_m(n) = \frac{\Delta G_m^*(n)}{RT} + \frac{z_m F}{RT} \phi(n) \tag{19}$$

It can be shown that the flux equations (*Eqns. 11 and 18*) are completely equivalent in the case of a very large number $N + 2$ of rate-limiting barriers. It is also found from both descriptions that a driving force, given here by the difference of electrochemical activities, is always required for inducing membrane transport. Hence, an asymmetric membrane is not capable of accomplishing *per se* a transport of permeants, which is at variance with *Deutsch's* suggestion [16]. However, as long as the rate-determining barriers of the relative height $\Delta G_m^*(n)/RT$ are not distributed symmetrically around the center of the membrane, such a system should generally exhibit different ion permeabilities (ionic conductances) in different directions (see *Fig. 3*). This is not only true for membranes

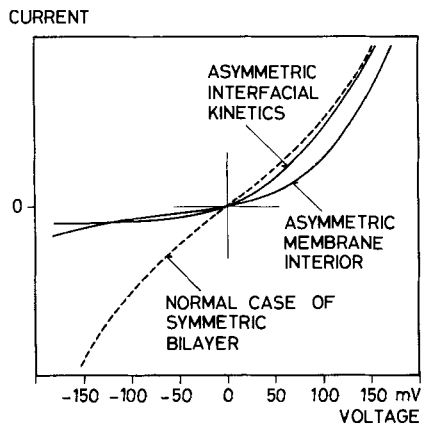


Fig. 3. Current-voltage curves for symmetric and asymmetric bilayer membranes in the presence of ionophores. Symmetric curve: normal case found for $Ca^{2+}/ETH\ 1001$ and K^+ /monactin [8][13]. Asymmetric curves: calculated for asymmetric membrane-internal barriers ($\Delta\Delta G_m^(n) = 2 RT$) and for kinetic limitations at one interface. Details of the calculations are given in [17].*

containing ion-selective carriers but also for membranes with channels since the basic flux Eqn. 18 does not involve any assumptions on the nature of the decisive energy barriers that must be surmounted by the permeating species.

Results and Discussion. – It was shown earlier [8–10] [13] [18] [19] that one given ion carrier may prefer divalent cations (*e.g.* Ca^{2+}) when applied in membrane media of relatively high dielectric constants, but becomes selective for monovalent cations (*e.g.* Na^+) in less polar environments. This is a consequence of the electrostatic interaction between the charged carrier complexes and the surrounding medium. Relations of the following type were derived for the $\text{Na}^+/\text{Ca}^{2+}$ selectivity of neutral carriers in membranes

$$\log K_{\text{CaNa}} \approx a + b \cdot \frac{1}{\varepsilon}$$

where ε is the dielectric constant of the membrane. Correspondingly, artificial bulk membranes with asymmetric selectivity properties were realized by simply combining two PVC-membrane moieties that incorporate the same ionophore, *N,N'*-bis[(11-ethoxycarbonyl)undecyl]-*N,N'*,4,5-tetramethyl-3,6-dioxaoctanediamide (*ETH 1001*) or *N,N'*-diheptyl-*N,N'*-dimethyl-3,6-dioxaoctanediamide (*ETH 64*) in a polar and a nonpolar plasticizer, respectively.

For assessing the potentiometric selectivity behavior, these membranes were mounted into ion-selective electrode cells, and EMF values were measured on separate sample solutions of Ca^{2+} and Na^+ ions. Figs. 4 and 5 show the resulting selectivity coefficients $K_{\text{CaNa}}^{\text{Pot}}$, as obtained from Eqns. 5 and 6. Evidently, freshly prepared asymmetric membranes yield widely different $\text{Na}^+/\text{Ca}^{2+}$ selectivities, depending only on which side of the membrane (polar or nonpolar) is exposed to the sample solution. As expected, the observed ion selectivities closely agree with the corresponding values determined for homogeneous polar or nonpolar membranes (see Figs. 4 and 5).

With increasing measuring time, however, the two-segmented membranes are found to gradually lose their initial asymmetry behavior, and the $\text{Na}^+/\text{Ca}^{2+}$ selectivities in Figs. 4

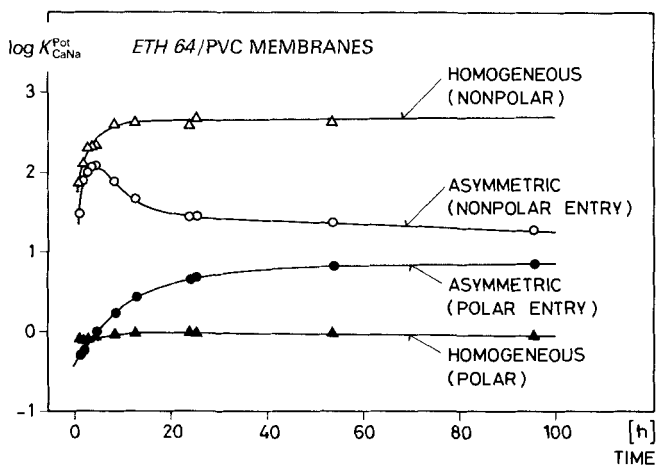


Fig. 4. Potentiometric $\text{Na}^+/\text{Ca}^{2+}$ selectivities ($\log K_{\text{CaNa}}^{\text{Pot}}$) of freshly prepared 800- μm thick asymmetric and homogeneous PVC membranes containing the neutral carrier ETH 64

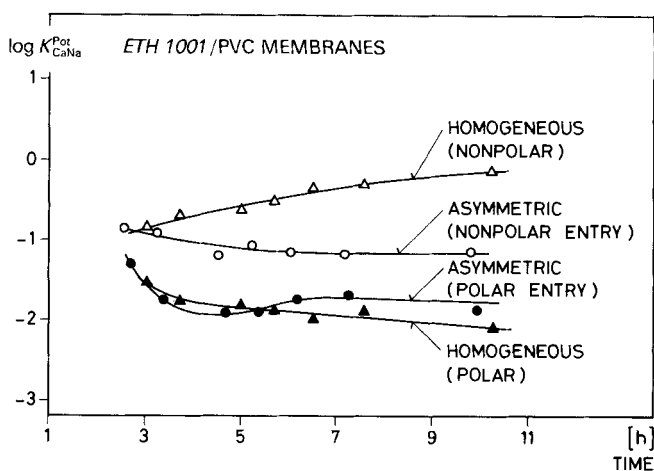


Fig. 5. Potentiometric $\text{Na}^+/\text{Ca}^{2+}$ selectivities ($\log K_{\text{CaNa}}^{\text{Pot}}$) of freshly prepared 600- μm thick asymmetric and homogeneous PVC membranes containing the neutral carrier ETH 1001

or 5 finally converge on the same level. The reason is that the plasticizer of one half-membrane can freely diffuse into the other, until this mutual mixing of polar and nonpolar plasticizers has led to a perfectly homogeneous membrane of intermediate dielectric properties. The selectivity changes set in as soon as the plasticizer of one membrane segment reaches the opposite membrane boundary. Since the diffusion coefficient D of plasticizers in PVC membranes (~ 40 wt.-% PVC) is of the order of 10^{-8} cm^2/s [20] and the thickness δ of each half-membrane is about 0.04 cm, one calculates a diffusion time of

$$\tau_{\text{diff}} = \frac{\delta^2}{2D} \approx 20 \text{ h},$$

which agrees with the experimental findings in Figs. 4 and 5. Accordingly, the studied composite membranes exhibit asymmetry behavior at best for a few hours after their assembly. This is, however, a sufficient time for performing ion transport experiments at applied voltages V of about 15 V because the driving force for ion migration then exceeds the driving force for diffusion by two orders of magnitude. The corresponding mean migration time for ions I^z in the half-membrane is found to be

$$\tau_{\text{migr}} = \frac{\delta^2}{2D_1} \cdot \frac{4RT}{z_1 FV} \approx 5 \text{ min}$$

Based on the previous results, it was expected that the two-segmented membranes containing the neutral carrier ETH 1001 or ETH 64 should yield a preferential electroanalytic transport of Ca^{2+} ions if the polar membrane boundary is offered on the entry side, whereas Na^+ ions should be favored by the nonpolar membrane boundary. These expectations were partly confirmed by preliminary experiments [21] (see Fig. 6). Although the observable effects are less pronounced than expected, the data unambiguously corroborate the asymmetric ion-transport behavior of the model membrane. Thus, the numbers n_{Ca} of moles of Ca^{2+} transferred into the cathode compartment as well as the electric transport numbers $t_{\text{Ca}} = 2F n_{\text{Ca}}/Q$ (Q : number of coulombs passed through the membrane) are significantly different after 2–3.5 h of electro dialysis on two identical but

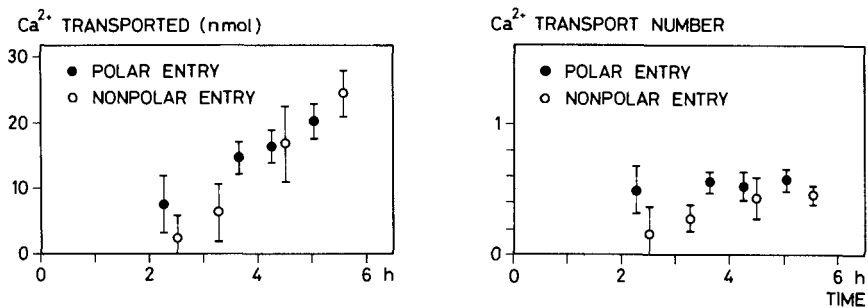


Fig. 6. Transport of Ca^{2+} ions across 400- μm composite membranes containing the neutral carrier ETH 1001 (applied voltage 15 V). The amount of Ca^{2+} transferred into the cathode compartment and the transport number t_{Ca} are given as a function of time. Polar half-membrane: carrier 3 wt.-%; *o*-nitrophenyl octyl ether 60 wt.-%; PVC 37 wt.-%. Nonpolar half-membrane: carrier 3 wt.-%; DNP 60 wt.-%; PVC 37 wt.-%.

reversely arranged membranes. On the other hand, the transport numbers obtained for Ca^{2+} ions entering at the polar membrane side are clearly below 1.0, which implies that other ions are also carried through the membrane, especially during the first period of measurements. Practically no transference of Ca^{2+} ions is found, however, when the two membrane moieties are separated by a thin diaphragm (see Fig. 7).

Now, Fig. 7 reveals that a preferential transport of Na^+ ions occurs in the early stage of the experiments even when the polar half-membrane is offered on the entry side. These results were quite unexpected but can be rationalized on the basis of the preceding theoretical considerations (see Fig. 2). Thus, it was found that the resistivity of the nonpolar membrane material exceeds that of the polar one by a factor of $\sim 10^2$. Accordingly, it is the nonpolar low-permeability membrane region that mainly determines the transport selectivity during the first period of measurements. With increasing measuring

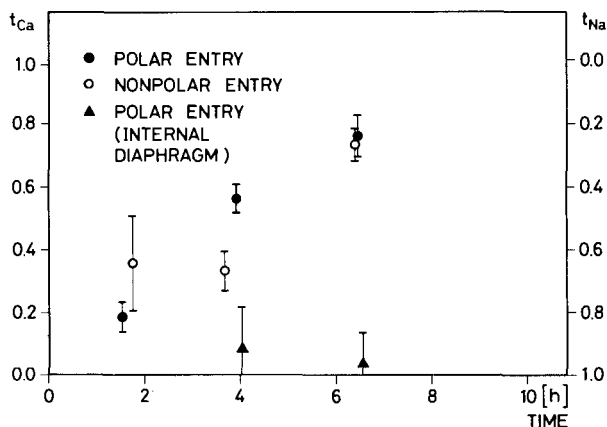


Fig. 7. Relative transport numbers, t_{Ca} and t_{Na} , observed in electrodiolytic ion-transport studies on asymmetric composite PVC membranes containing the neutral carrier ETH 1001. Two-segmented membranes with the polar or the nonpolar moiety exposed to the sample solution on the anode side, and a three-segmented membrane (additional internal diaphragm) with the polar entry side were used for the experiments. The measured transport numbers for Ca^{2+} (left scale) and for Na^+ (right scale) are given relative to their sum.

time, diffusion of the polar plasticizer into the nonpolar half-membrane evidently lowers the membrane resistance (except for the experiment with the separating diaphragm). This permits asymmetric selectivity behavior of the membrane to be observed even in electro-dialysis studies. The asymmetry phenomena obviously disappear after > 5 h, when the diffusion- and electroosmosis-controlled mutual mixing of the two plasticizers is more complete. Finally, each membrane surface prefers Ca^{2+} over Na^+ ions both in potentiometric and in transport experiments (see *Figs. 5–8*).

Although the asymmetry phenomena observed in electro-dialytic studies on composite membranes are less pronounced than the results achieved potentiometrically, the effects

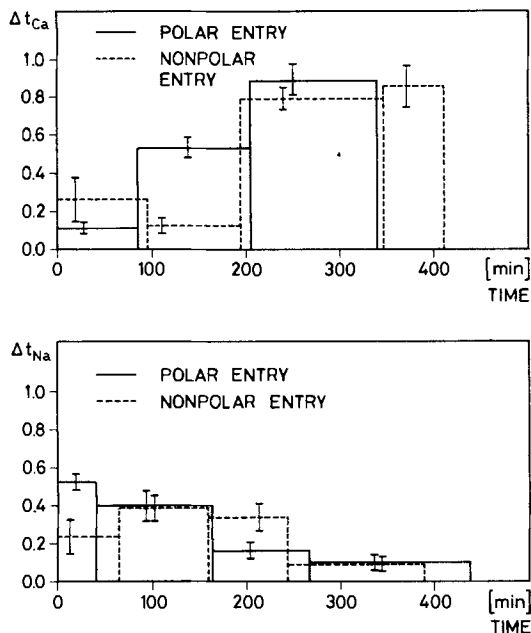


Fig. 8. Actual transference numbers, Δt_{Ca} and Δt_{Na} , representative for given time intervals of electro-dialysis on asymmetric composite membranes (neutral carrier *ETH 1001*). The values Δt_i indicate the contribution of the species i to the total charge increment ΔQ transferred through the membrane.

become quite evident from *Fig. 8*. It illustrates the actual ionic transport numbers Δt_{Ca} and Δt_{Na} determined during given time periods of electro-dialysis. There is no doubt that one given ionophore, operating in an asymmetric membrane, can be capable of mediating a selective transport of different ions in different directions. In other words, the observed permeability of such bulk membranes for a given species depends on the direction of ion transport, *i.e.*, on the direction of the applied driving forces. A very similar behavior was found for asymmetric lipid bilayers containing ion-selective channels [1–4] or carriers [2]. Here, in agreement with theoretical predictions, the direction-dependent permeability for substrate ions results in asymmetric current-voltage curves (rectification phenomena, see *Fig. 3*).

It can be concluded that membranes with ideally asymmetric transport properties can produce an enrichment of certain permeating species on one side when they are exposed to oscillating or fluctuating driving forces. It is well conceivable that the principle of asymmetric membranes is often applied in biological systems in order to maintain or even establish asymmetries in the external solutions with minimal consumption of energy.

Experimental Part

Membrane Preparation. – Dinonyl phthalate (DNP; for GC *Merck*) was used as plasticizer for the nonpolar PVC membrane segments, whereas the polar segments contained *o*-nitrophenyl dodecyl ether (*o*-NPDE; synthesis below) or *o*-nitrophenyl octyl ether (*Fluka*; see Fig. 6). Two types of asymmetric composite membranes were used: a) For ion transport and EMF measurements, the composition of the polar half-membrane (thickness: 0.4 mm) was 1.5 wt.-% ionophore (*ETH 1001*; *Fluka*), 60 wt.-% *o*-NPDE, and 38.5 wt.-% PVC (SDP, high molecular, *Lonza*), and the composition of the nonpolar half-membrane (thickness: 0.2 mm) was 1.5 wt.-% *ETH 1001*, 60 wt.-% DNP, and 38.5 wt.-% PVC. b) For some EMF measurements, membranes were prepared from two 0.4-mm thick half-membranes containing 3 wt.-% *ETH 64* (1 in [22]), 60 wt.-% *o*-NPDE or DNP, and 37 wt.-% PVC.

The membrane segments were prepared as described in [23]. Each membrane segment was equilibrated separately for at least 12 h: for transport experiments in 10^{-2} M RbCl, and for EMF measurements in a mixed soln. of $5 \cdot 10^{-2}$ M CaCl₂ and $5 \cdot 10^{-2}$ M NaCl (all salts from *Merck*). Then the contacting surfaces of the half-membranes were washed (H₂O), dried (filter paper), and clamped together.

Transport Experiments. – *Cell Assembly.* The electro dialysis cell consisted of two electrolyte compartments, each of ca. 30 ml, separated by the cation-selective membrane. The diameter of the active membrane area was 4 cm. Both compartments were equipped with Pt disk electrodes (diameter: 4 cm) and with magnetic stirrers.

Procedure. All measurements were performed at r.t. For the determination of the cation transport numbers, the anode compartment was filled with a soln. of $5 \cdot 10^{-3}$ M CaCl₂ and $5 \cdot 10^{-3}$ M NaCl, whereas a soln. of 10^{-2} M RbCl was used in the cathode compartment. The system was leak-tested for 1 h. Then a constant voltage of 15 V was applied over the membrane, resulting in an electric current of about 1 μA. The concentrations of Ca²⁺ and Na⁺ ions transported into the cathode compartment were determined by flameless atomic-absorption spectrometry (*IL 551*, with furnace atomizer *IL 655*; *Instrumentation Laboratory*, Wilmington, MA 01887, USA). To this end, 4 samples of 10 μl were collected and analyzed every 20 to 60 min. Before and after each measurement the spectrometer was calibrated. The standard deviation of the measured concentrations was 2–8%. Finally the transport numbers for Ca²⁺ and Na⁺ ions were calculated from the charge equivalent of the transferred species and the current-time integral.

EMF Measurements. – *Cell Assembly.* The measurements were performed on cells of the type Hg; Hg₂Cl₂, KCl (sat.) | 3M KCl | sample solution || membrane system || $5 \cdot 10^{-2}$ M CaCl₂, $5 \cdot 10^{-2}$ M NaCl, AgCl; Ag. The external reference electrode was a double junction calomel electrode *Philips R44/2-SD/1*. The membranes were mounted in *Philips IS 561* electrode bodies.

Procedure. The EMF measurements were carried out at r.t. using *AD 515* operational amplifiers and *AD 510* differential amplifiers (*Analog Devices*, Norwood, MA 02062, USA). The selectivity factors were determined by the separate soln. method [24]. The activity coefficients used were taken from [8] [25]. The measured EMF values were corrected for changes in the liquid junction potential on the basis of the *Henderson* equation [8] [26]. To assess the selectivity factors as a function of the time, EMF values were alternately taken in 10^{-2} M CaCl₂ and 10^{-2} M NaCl solns.

o-Nitrophenyl Dodecyl Ether (*o*-NPDE). 2-Nitrophenol (9.7 g, 0.07 mol; *puriss. p.a.*, *Fluka*), 1-bromododecane (19.17 g; *puriss. Fluka*), and K₂CO₃ (9.66 g; water-free, *puriss. p.a.*, *Fluka*) were added to 100 ml of acetone. The mixture was stirred at r.t. for 48 h, then heated under reflux for 120 h, and finally dried by evaporation. H₂O was added to the precipitate, and the mixture was extracted with Et₂O (3×). Then the Et₂O phase was extracted with 10% NaOH (3×), washed (H₂O), and dried (MgSO₄). Finally, the solvent was evaporated and the product was distilled (200°/0.1 Torr): 18 g (83%) of *o*-nitrophenyl dodecyl ether. The IR, ¹H-NMR, ¹³C-NMR and mass spectra are in agreement with the constitution of *o*-NPDE. Anal. calc. for C₁₈H₂₉NO₃ (307.43): C 70.32, H 9.51, N 4.56; found: C 70.36, H 9.61, N 4.56.

REFERENCES

- [1] H.-J. Apell, F. Bamberg, H. Alpes, P. Läuger, *J. Membr. Biol.* **1977**, *31*, 171.
- [2] O. Fröhlich, 'Untersuchungen an künstlichen Bilayermembranen aus Lipidmonoschichten', Dissertation Univ. Konstanz, 1976.
- [3] J. L. Flagg-Newton, W. R. Loewenstein, *Science* **1980**, *207*, 771.
- [4] Ion transport across biological membranes and its control (International workshop, Maria Laach, FRG, Sept. 25–27, 1983); B. Deuticke, E. Hildebrand, J. Schnakenberg, H. Stieve, *FEBS Lett.* **1984**, *176*, 1.
- [5] W. Köhne, B. Deuticke, in ref. [4].
- [6] R. Krämer, in ref. [4].
- [7] W. Schwarz, R. Grygorcyk, in ref. [4].
- [8] W. E. Morf, 'The Principles of Ion-Selective Electrodes and of Membrane Transport', Adadémiai Kiadó, Budapest; Elsevier, Amsterdam, 1981.
- [9] D. Ammann, W. E. Morf, P. Anker, P. C. Meier, E. Pretsch, W. Simon, *Ion Selective Electrode Rev.* **1983**, *5*, 3.
- [10] W. E. Morf, W. Simon, in 'Ion-Selective Electrodes in Analytical Chemistry', Ed. H. Freiser, Plenum Press, New York–London–Washington–Boston, 1978, Vol. 1, pp. 211–286.
- [11] A. P. Thoma, A. Viviani-Nauer, S. Arvanitis, W. E. Morf, W. Simon, *Anal. Chem.* **1977**, *49*, 1567.
- [12] W. E. Morf, P. Wuhmann, W. Simon, *Anal. Chem.* **1976**, *48*, 1031.
- [13] W. E. Morf, D. Ammann, R. Bissig, E. Pretsch, W. Simon, in 'Progress in Macrocyclic Chemistry', Eds. R. M. Izatt and J. J. Christensen, John Wiley & Sons, New York–Chichester–Brisbane–Toronto, 1979, Vol. 1, pp. 1–61.
- [14] R. Schlögl, *Z. Phys. Chem. (Frankfurt am Main)* **1954**, *202*, 305.
- [15] P. Läuger, B. Neumcke, in 'Membranes', Ed. G. Eisenman, Dekker, New York, 1973, Vol. 2, pp. 1–59.
- [16] D. H. Deutsch, *Am. Lab.* **1981**, *13*, 54.
- [17] W. E. Morf, E. Pretsch, W. Simon, in 'Structure and Dynamics of Membranes, Nucleic Acid & Proteins', Eds. E. Clementi, G. Corongiu, M. H. Sarma, and R. H. Sarma, Adenine Press, Guilderland, New York, 1985, pp. 139–153.
- [18] U. Fiedler, *Anal. Chim. Acta* **1977**, *89*, 111.
- [19] W. Simon, W. E. Morf, E. Pretsch, P. Wuhmann, in 'Calcium Transport in Contraction and Secretion', Eds. E. Carafoli, F. Clementi, W. Drabikowski, and A. Margreth, North-Holland Publishing Company, Amsterdam–Oxford; American Elsevier Publishing Company, Inc., New York, 1975, pp. 15–23.
- [20] U. Oesch, W. Simon, *Anal. Chem.* **1980**, *52*, 692.
- [21] W. E. Morf, H. Ruprecht, P. Oggenfuss, W. Simon, in 'Ion Measurements in Physiology and Medicine', Eds. M. Kessler, J. Höper, and D. K. Harrison, Springer-Verlag, Berlin, 1985, in press.
- [22] E. Lindner, K. Tóth, E. Pungor, F. Behm, P. Oggenfuss, D. H. Welti, D. Ammann, W. E. Morf, E. Pretsch, W. Simon, *Anal. Chem.* **1984**, *56*, 1127.
- [23] G. J. Moody, R. B. Oke, J. D. R. Thomas, *Analyst* **1970**, *95*, 910.
- [24] W. Simon, D. Ammann, M. Oehme, W. E. Morf, *Ann. N.Y. Acad. Sci.* **1978**, *307*, 52.
- [25] P. C. Meier, *Anal. Chim. Acta* **1982**, *136*, 363.
- [26] P. C. Meier, D. Ammann, W. E. Morf, W. Simon, in 'Medical and Biological Applications of Electrochemical Devices', Ed. J. Koryta, John Wiley & Sons Ltd., Chichester, 1980, Chapter 2, pp. 13–91.